JOURNAL OF BIOMEDICAL OPTICS 2(3), 326–331 (JULY 1997)

THERMAL LENS DETECTOR SYSTEM FOR CAPILLARY ELECTROPHORESIS

Bernd Stefan Seidel, Werner Faubel, and Hans Joachim Ache
Forschungszentrum Karlsruhe, Institut für Instrumentelle Analytik, Postfach 3640, D-76021 Karlsruhe, Germany

(Paper JBO-126 received Nov. 14, 1996; revised manuscript received May 9, 1997; accepted for publication May 14, 1997.)

ABSTRACT

The characteristics and the performance of a thermal lens detector, which uses a double-beam absorption scheme, were studied in a capillary electrophoresis system with various types of toxic pollutants, e.g., pesticides. The setup of the detector system was miniaturized using the smallest diverging path lengths between the cell and the pinhole (4 mm). The probe laser beam (He:Ne laser, 633 nm) and the excitation beam (Ar^+ ion laser, 364, 457, 488, and 514 nm) with a crossed setup were directed by mirrors into two microscope objectives that focused the beam to a 5-μm waist inside the capillary. The detection volume was on the order of 75 nl when a 75-μm capillary was employed. The change in intensity of the probe beam was detected by a photodiode behind a pinhole, which was protected with different band-pass interference filters. The excitation laser can be used in the multiline order. Micellar electrokinetic methods are used for pesticide separation. The performance of the detector in capillary electrophoresis was assessed with various types of capillaries and compared with a conventional absorption detector. The limit of detection is at least one order of magnitude better than it is with the absorption detector. © *1997 Society of Photo-Optical Instrumentation Engineers.* [S1083-3668(97)01003-4]

Keywords laser; thermal lens; photothermal methods; capillary electrophoresis; small volumes.

1 INTRODUCTION

Capillary electrophoresis[1,2] is a microvolume separation technique increasingly achieving recognition for use in the separation of inorganic and organic compounds, especially in mixed biomedical samples. The key features of the method are its very short analysis time, and sample volumes in the nanoliter and picoliter range. Separation efficiency is influenced mainly by the inner diameter of the capillary, which is usually on the order of 10 to 200 μm. Many detection methods are combined with capillary electrophoresis (CE), e.g., ultraviolet-visible spectrophotometry (UV-VIS absorption), fluorescence, electrochemistry, and mass spectrometry.[1] UV-VIS absorption detection is the most common method. However, the limit of detection (LOD) is not satisfactory because the optical path length inside the capillary is too short. Another spectroscopic technique is laser fluorescence spectroscopy, one of the most sensitive optical methods, but not always suitable, as not all molecules exhibit fluorescence. In an additional step, nonfluorescent molecules can be labeled so as to fluoresce, but this requires sample pretreatment, which is cumbersome. Photothermal techniques[3] thus have some important advantages to offer in detection devices.

Address all correspondence to Bernd Stefan Seidel. Phone: 49 7247 822662; Fax: 49 7247 824618; E-mail: bernd.seidel@ifia.fzk.de

2 PHOTOTHERMAL METHODS

2.1 BASIC PRINCIPLES

The idea underlying photothermal methods is this: An excitation light beam passes through the sample of interest; the light is tuned to an absorption line of the analyte; and the optical energy is absorbed by the medium. If the collisional quenching rate in the analyte is significantly higher than the radiative rate, most of the energy appears in the electronic states or vibrational and rotational-translation modes of the molecules. Heating the medium changes the refractive index. The change in the refractive index of the medium can be detected either directly by means of an interferometer (photothermal phase-shift spectroscopy or photothermal interferometry), or by a probe laser beam that changes its shape (converging or diverging) (thermal lensing) or is deflected (photothermal deflection spectroscopy) when passing the region excited by the pump beam. In photoacoustics, a microphone for gases and solids or a piezoelectric transducer for liquids, which are in acoustic contact with the sample, are used as detectors to measure the amplitudes of the resultant acoustic waves.

The photothermal effect can be monitored as a change in intensity of the probe beam by a photodiode after passing through a pinhole (thermal lensing, TL), or by a position-sensitive detector as a deflection of the probe laser beam (photothermal

deflected spectroscopy, PDS) caused by the change in refractive index behind the sample cell. The distance between the sample and the pinhole determines the size of the detector. For practical application, we succeeded in shortening the distance between the pinhole and the sample cell from the typical 400 mm to 4 mm. The latest experiments with the so-called near-field thermal lens were performed with a newly constructed rugged and compact system that is easy to use with a capillary electrophoresis system.

Photoacoustic and photothermal techniques, such as photoacoustic spectroscopy (PAS), thermal lensing, photothermal deflection spectroscopy, and photothermal phase-shift spectroscopy (PTPS), have proved in the past few years to be valuable analytical tools for measuring very small concentrations of analytes in liquids. PAS especially is preferred in analytical measurements to photothermal techniques, because very fast and easy alignment procedures allow it to be used sporadically. Our own experimental studies of the performance of the four related techniques mentioned above have shown photothermal techniques to be superior to PAS and conventional spectrophotometry in assays for environmental pollutants.[4]

2.2 THERMAL LENSING

Thermal lensing was reported first by Gordon et al.[5] They accidentally observed the TL effect during the study of laser Raman scattering. They put a sample cell of 1-cm path length into the cavity of an He:Ne laser and, noticing the change in thermo-optical properties, 1 year later proposed TL as a method for measuring small absorption coefficients.[6] The first dual-beam experiment was conducted by Grabiner Siebort and Flynn[7] in 1972 with a CO_2 laser as pump beam and a continuous He:Ne laser as probe beam. They observed the change in the refractive index caused by heating from vibrational relaxation processes of gases at a reduced pressure. This marked the first activity in trace analysis in gases.

Hu and Whinnery[8] optimized the TL signal by positioning the probe beam waist one confocal length in front of the minimum beam waist of the pump beam. Most of the thermal lens instruments described are based on far-field detection. This is a major drawback because the setup needs long deflection path lengths on the order of a few meters. Miniaturization of thermal lens instruments began with the development of the so-called near-field detection by Power[9] and Long and Bialkowski.[10] It now became possible to build miniaturized sensor systems that were easy to align.[11,12]

The theory of the thermal lens effect has been described frequently and was summarized in monographs edited by Kliger in 1983[13] and by Mandelis in 1992.[14] Briefly, the models include various different excitation sources, various geometries of the pump and probe beams (collinear, transverse, or shifted by a small angle) and flow of the observed media. Figure 1 shows the typical detection device for a thermal lens in combination with capillary electrophoresis. The laser light is condensed and impinges into the capillary (inner diameter between 200 and 25 μm) containing the sample solution. A modulated pump beam produces the time-dependent thermal lens. A transverse probe beam detects the lens by changing its intensity, which is measured with a calibrated photodiode behind a pinhole.

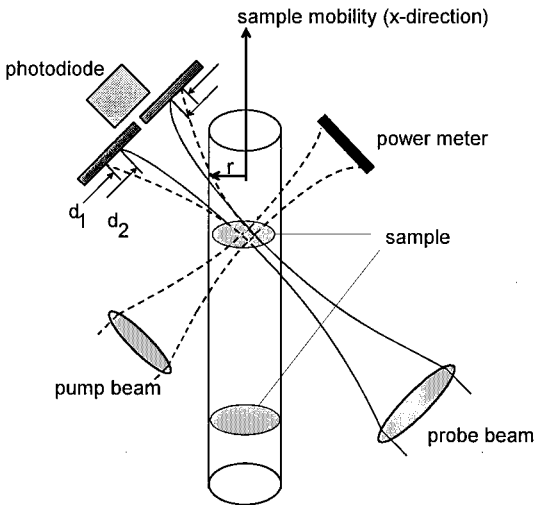

Fig. 1 Schematic view of the thermal lens effect, transverse dual beam setup; d_1 and d_2 indicate the He:Ne laser probe beam diameters without and with thermal lens excitation, respectively.

The thermal lens signal on the photodiode depends on the refractive index profile induced in the sample by the pump beam. Under equilibrium conditions, the temperature change is related to the refractive index through the differential equation[13]:

$$dn/dT = (\partial n/\partial T)_p + (\partial n/\partial \rho)(\partial \rho/\partial T)_p, \quad (1)$$

where n is the refractive index, T is the temperature, p is the pressure, and ρ is the density.

In practice, the thermal lens signal $S(t)$ is a time-dependent function of the probe laser beam intensity. The intensity change of the probe beam in the presence of the thermal lens, $I_T(t)$, relative to the initial value, $I_T(t=0)$, can be expressed by the following equation:

$$S(t) = I_T(t) - I_T(t=0)/I_T(t=0). \quad (2)$$

3 EXPERIMENTAL

This section discusses the application of thermal lensing as a miniaturized detector system for capillary electrophoresis. The path length inside the capillary is given by the diameter of the capillary, which is between 25 and 200 μm. Transverse arrangement of both laser beams is recommended be-

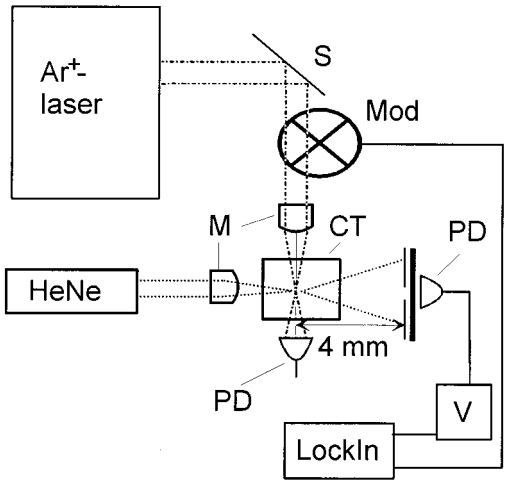

Fig. 2 Schematic setup of the CE-TL detector. S, mirror; Mod, chopper or acousto-optic modulator; M, microscope objective; CT, capillary tube; PD, photodiode; HeNe, helium neon laser; V, preamplifier; LockIn, LockIn-amplifier.

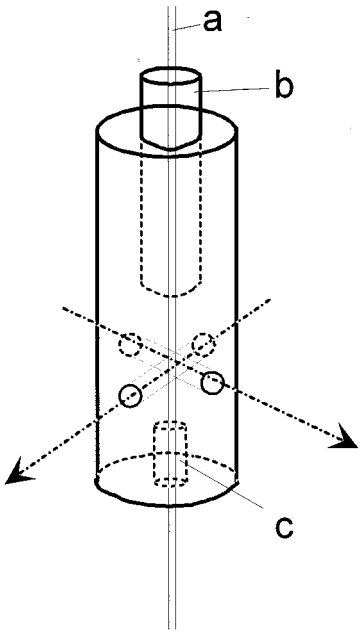

Fig. 3 Sketch of a self-made capillary stage. a, capillary; b, holder; c, center socket; the two arrows indicate the laser light beams.

cause the path length is of the same magnitude, but additional noise by the collinear setup is avoided. A comparison of the signal-to-noise ratio for collinear and transversal thermal lensing is given by Georges.[15] He showed that the signal-to-noise ratio for optical path lengths smaller than 500 μm with the crossed-beam setup is improved. Figure 2 shows the schematic setup of the CE detector system. An Ar^+ laser (Innova 200, Coherent) is used for a pump beam. This laser system delivers up to 800 mW of cw light at $\lambda = 364$ nm, but only 150 mW are used. The wavelength is suitable for the detection of nitrophenol pesticides in aqueous solutions. The beam is intensity modulated by a chopper or an acousto-optic modulator, which simultaneously gives the reference signal of the lock-in amplifier to permit phase-sensitive detection. The beam is focused inside the capillary with a 5× microscope objective, which changes the refractive index of the flowing medium. A second intensity-stabilized helium:neon laser is used to detect the change in the refractive index. Another 5× microscope objective focuses the beam to a spot of 5 μm diameter inside the capillary and overlaps it with the pump beam to obtain the maximum thermal lens signal. The probe beam diverges after the capillary, and the TL signal is detected by a photodiode behind a pinhole, only 4 mm behind the capillary. The TL signal is preamplified and fed to a lock-in detector. Another photodiode records the intensity of the pump beam and is used for standardization.

The capillary stage, CT, shown in Figure 3, when combined with the Spindler and Hoyer microbank system, allows three-dimensional alignment of the beams to be achieved with a precision in the micrometer range.[12]

The alignment procedure requires a walk-in procedure to be performed for the best TL signal. First, the probe beam is adjusted, then the position of the pump beam is aligned and the TL signal optimized.

3.1 APPLICATION TO CAPILLARIES WITH SMALL INNER DIAMETERS

One of the biggest disadvantages in UV/VIS electrophoresis with very small capillaries is the incoherent light source. Therefore, laser systems are preferable when an extremely highly focused beam waist, in the micrometer range, of high intensity is required. Another disadvantage is the small optical path length inside the capillary. Absorbance spectroscopy is based on the Lambert–Beer law. When a very sensitive device is required, the optical path length should be large. This is in contrast to separation conditions, which improve with smaller diameters. The crossed-beam thermal lens allows miniaturization, because the optical path length is given by the overlap of both beams, which is independent of the capillary diameter.

Electrophoretic separations were performed in fused silica capillaries with 50 to 250 μm i.d. (Bischoff Analysensysteme, Leonberg, Germany). The detection window was placed in the middle of an 80-cm long capillary. The effective length was only 40 cm. Before each measurement, the capillaries were treated with 1*N* NaOH, 0.1*N* NaOH, H_2O, and the buffer system. The samples were injected hydrodynamically, electrophoretic injection being unsuited for nonpolar substances. The injection conditions for all capillaries were 1 s under vacuum, corresponding to different injection volumes. Table 1 shows the dependence of the probe volume on the diameter of the capillaries. Owing to

Table 1 Features of capillaries.

Inner diameter (i.d.) (μm)	Injection volume (capillary of 1 m length)	Volume of capillary (capillary of 1 m length)	Relative resistance
250	49 nl	49 μl	625%
100	7.9 nl	7.9 μl	100%
75	4.4 nl	4.4 μl	56%
50	2.0 nl	2.0 μl	25%
25	0.5 nl	0.5 μl	6%

the electric field of the CE system, a current is introduced inside the capillary. This current depends on the following parameters:

$$P = UI = RI^2 = U^2 d^2 \frac{\pi\kappa}{2L}, \tag{3}$$

where P is power [W], U is voltage [V], I is amperes [A], R is resistance [Ω], d is diameter of the capillary [m], and U, κ is thermal conductivity [W/mK]. The relative resistance, which is set to 100% for a 100-μm capillary, is an indication of the resistance of the capillary. The resistance becomes lower by a factor of 4 when the i.d. of the capillary is bisected. In this way Joule heating is reduced by a factor of 4, and the conductivity is improved by the higher surface-to-volume ratio as shown in Figure 4.

Small internal diameters of capillaries are advantageous because Joule heating is reduced faster by a higher surface-to-volume ratio. However, the thermal lensing detector system supports the use of very small capillaries because the detection limit is not influenced by the smaller diameter of the capillaries. Figure 5 shows the role of the capillary diameter with current-voltage curves. The curves for the smallest diameter (25 and 50 μm) exhibit linearity

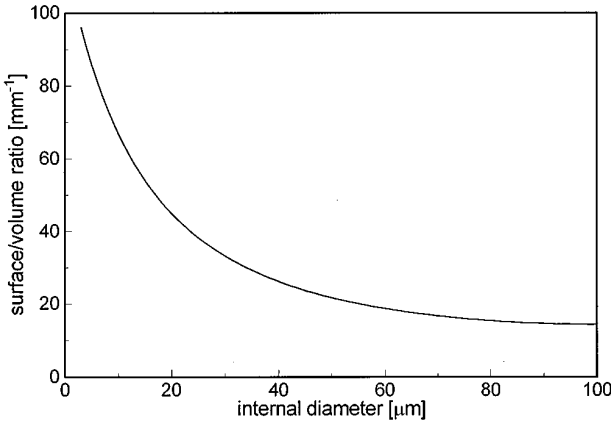

Fig. 4 Surface-to-volume ratio as a function of the capillary diameter.

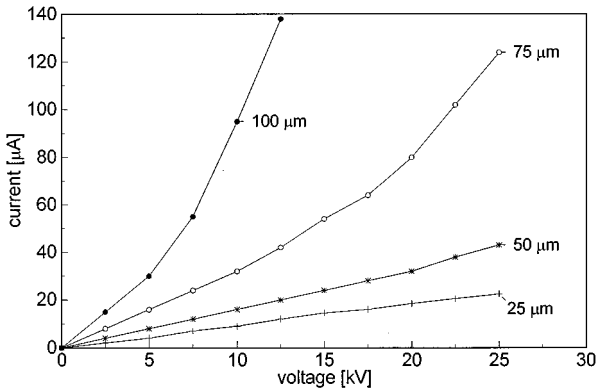

Fig. 5 Ohm's law plot for an anionic buffer of various capillary diameters.

over the entire voltage range, as expected in accordance with Ohm's law. The capillaries with large diameters show increased resistance at higher voltages due to the lower thermal conductivity of the wall.

However, the miniaturization of the geometry is limited by the spot size of the probe beam. If the waist of the beam is the size of the capillary diameter, the beam is diffracted, and interference fringes are produced. In Figure 6, the interference fringes are shown for a 25-μm capillary and a focused He:Ne laser. Taringen et al.[16] used this effect for measuring refractive index. A slit is adjusted between two maxima and the change in intensity is measured.

3.2 SEPARATION OF PESTICIDES

There is a great interest in detecting pesticides in the parts for billion range[17] because of their toxicity to humans. Different separation principles (e.g., micellar electrokinetic capillary chromatography) allow the separation of relatively unpolar pesticides. In this work, a group of nitrophenol pesticides were investigated. The pesticides separated are shown in Figure 7.

Micellar electrokinetic capillary chromatography (MECC) allows unpolar samples to be separated by a distribution of the substances between the aqueous electrophoretic buffer phase as carrier electrolyte and the micelles (pseudostationary phase), which arise when the concentration of the surfactant is higher than the critical micellar concentration. This method was described first by Terabe et al. in 1984.[18] The pesticides were separated by

Fig. 6 Interference pattern produced by focusing an He:Ne laser through a 25 μm capillary.

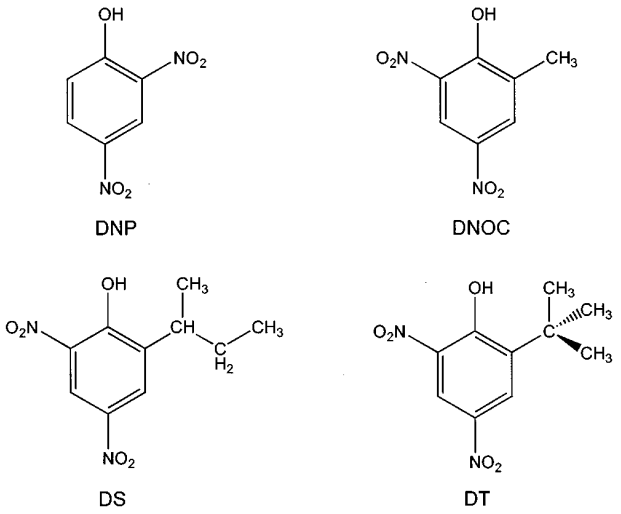

Fig. 7 Nitrophenol pesticides; DNP, 4,6-dinitrophenol; DNOC, 2-methyl-4,6-dinitrophenol; DS, 2-sec-butyl-4,6-dinitrophenol (dinoseb); DT, 2-tert.-butyl-4,6-dinitrophenol (dinoterb).

MECC and detected with a UV-VIS detector (linear UVIS 200, Thermo Separation Products) and the TL detector system. The anionic surfactant used was sodium dodecyl sulfate (SDS), which is an anionic detergent. As a carrier electrolyte, 50 m*M* SDS, 10 m*M* Na-phosphate was used with pH=7.0. In Figure 8, the separation by the UV detector is shown; in Figure 9, the TL detector is used. The signal-to-noise ratio is significantly improved by the TL detector, thus allowing detection in the parts per billion range. The UV detector was fixed at a wavelength of 364 nm±3 nm; the pump beam of the TL detector delivered a power of 150 mW.

Figures 10 and 11 show the calibration curves of both detectors. The linearity of both methods for a 75 μm capillary is more than three orders of magnitude. The limit of detection with a signal-to-noise ratio of 3 is 1.1 ppm for DNOC for the UV-VIS absorbance detector and 23 ppb for the TL detector, which is a factor of 48 less than in usual absorbance spectroscopy.

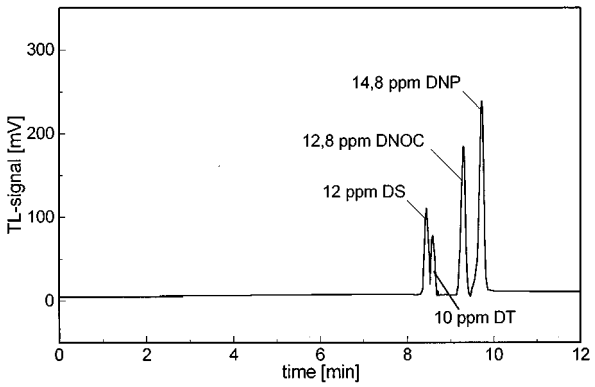

Fig. 9 Capillary electropherogram of a mixture of pesticides with TL detection with a 75 μm capillary.

In Table 2 the effect of different dimensions of capillaries is presented for the UV absorbance detector and the TL detector. As expected, the thermal lens reveals its superiority over the UV absorbance detector by shortening the optical path length inside the capillary. The UV absorbance detector follows the Lambert–Bes law: at a capillary diameter of 200 μm, the limit of detection for DNOC is 405 ppb and at a diameter of 100 μm, the LOD nearly doubles to 815 ppb. If the diameter is decreased from 100 μm to 50 μm, the LOD increases by a factor of 3 (815 ppb to 2550 ppb), which is caused by the stray light inside the capillary; this means that a part of the light beam does not cross the buffer zone of the capillary. The other part is guided by the glass wall to the photodetector without any absorption with the sample.

The thermal lens is independent of the capillary diameter in the range of 200 and 75 μm. If capillaries are used that are smaller than 50 μm, the signal-to-noise ratio is increased and the LOD for DNOC incrases from 23 to 45 ppb.

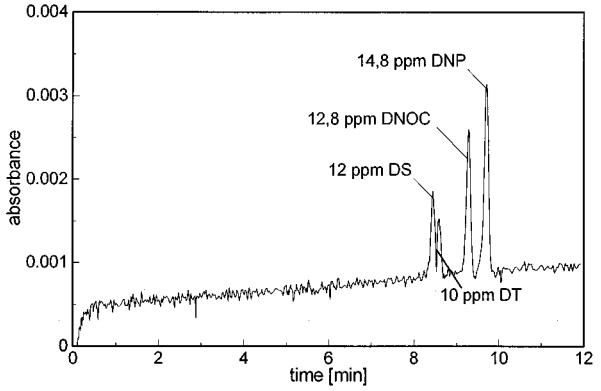

Fig. 8 Capillary electropherogram of a mixture of pesticides with UV absorbance detection with a 75 μm capillary.

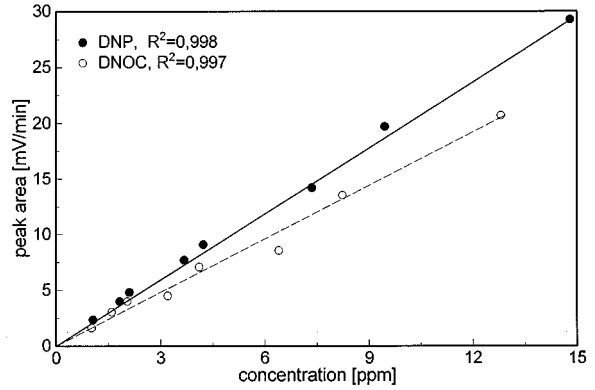

Fig. 10 Calibration curve of the pesticides DNOC and DNP with the UV-VIS absorbance detector.

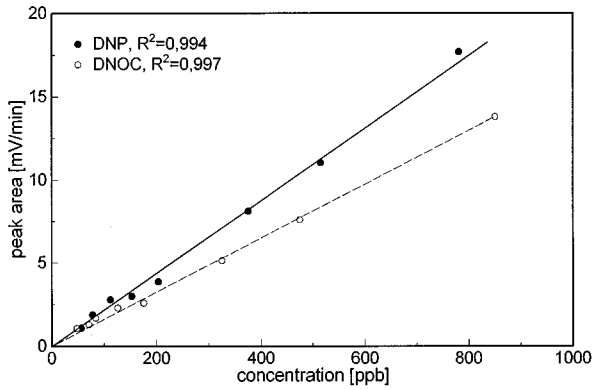

Fig. 11 Calibration curve of the pesticides DNOC and DNP with the TL detector.

4 CONCLUSIONS

We have shown that thermal lens in combination with capillary electrophoresis can perform separations of pesticides with high sensitivity. The crossed-beam setup of the detector system allows very small capillaries to be used because the optical interaction path length is not shortened, in contrast to normal absorbance measurements. The diameter of the capillary is limited only by the optical alignment of the beams. If the diameter is on the order of the waist of the probe beam, interference fringes must be analyzed, which limits the range of calibration. Therefore, absorbance measurement by thermal lens is limited by the smallest focusing system used for the probe beam.

In the future, this system will be combined with a laser-induced fluorescence system. Then it will be possible to detect all substances showing absorbance in the spectral range under observation. In combination with indirect detection methods, this capillary systems allows trace analysis of biomedical and biochemical substances in the smallest detection volumes.

Table 2 Comparison of limit of detection for the UV absorbance detector and TL detector as a function of capillary diameter.

Diameter of capillary (μm)	UV-VIS detector (ppb)	TL (ppb)
200	405	23
100	815	23
75	1100	23
50	2550	45

Acknowledgment

The authors are grateful to Hewlett Packard, Waldbronn, Germany, for technical support and helpful discussions.

REFERENCES

1. H. Engelhardt, W. Beck, and T. Schmitt, *Kapillarelektrophorese*, Vieweg, Braunschweig, Wiesbaden, (1994).
2. P. Jandik and G. Bonn, *Capillary Electrophoresis of Small Molecules and Ions,* VCH, Weinheim (1993).
3. A. Rose, R. Vyas, and R. Gupta, ''Pulsed photothermal deflection spectroscopy in a flowing medium: a quantitative investigation,'' *Appl. Opt.* **28**, 2554–2561 (1989).
4. W. Faubel, T. Schulz, B. S. Seidel, E. Steinle, and H. J. Ache, ''Comparing the analytical potential of PAS, PDS, TL and PTPS for trace detection in water,'' *J. Phys. IV* **C7**, 531–534 (1994).
5. J. P. Gordon, R. C. C. Leite, R. S. Moore, S. P. S. Porto, and J. R. Whinnery, ''Long-transient effects in lasers with inserted liquid samples,'' *Bull. Am. Phys. Soc.* **9**, 501 (1964).
6. J. P. Gordon, R. C. C. Leite, R. S. Moore, S. P. S. Porto, and J. R. Whinnery, ''Long-transient effects in lasers with inserted liquid samples,'' *J. Appl. Phys.* **36**, 3–8 (1965).
7. F. R. Grabiner, D. R. Siebart, G. W. Flynn, ''Laser induced time dependent thermal lensing studies of vibrational relaxation: translational cooling in CH_3F,'' *Chem. Phys. Lett.* **17**, 189–194 (1972).
8. C. Hu, and J. R. Whinnery, ''New thermooptical measurement method and a comparison with other methods,'' *Appl. Opt.* **12**, 72–79 (1973).
9. J. F. Power, ''Pulsed mode thermal lens effect detection in the near field via thermally induced probe beam spatial phase modulation: a theory,'' *Appl. Opt.* **29**, 52–63 (1990).
10. G. R. Long and S. E. Bialkowski, ''Pulsed infrared laser thermal lens spectrophotometric determination of trace-level gas-phase analytes: quantitation of parts per billion dichlorodifluoromethane,'' *Anal. Chem.* **56**, 2806–2811 (1984).
11. B. S. Seidel, *Die photothermische Interferometrie als miniaturisiertes Detektorsystem für Schadstoffe in Flüssigkeiten und Gasen*, Wissenschaftliche Berichte, FZKA 5697 Forschungszentrum Karlsruhe (1996).
12. E. Steinle, *Die Thermische Linse als Detektorsystem für die Kapillarelektrophorese und die Hochleistungsflüssigkeitschromatographie*, Wissenschaftliche Berichte, FZKA 5823 Forschungszentrum Karlsruhe (1996).
13. H. L. Fang and R. L. Swofford, ''The thermal lens in absorption spectroscopy,'' in *Ultrasensitive Laser Spectroscopy*, D. S. Kliger, Ed., Academic Press, New York (1983).
14. R. Gupta, ''Principles of Photothermal spectroscopy in fluids,'' *Principles and Perspectives of Photothermal and Photoacoustic Phenomena*, A. Mandelis, Ed., Progress in Photothermal and Photoacoustic Sciences and Technology, Vol. 1, pp. 96–154, Elsevier, New York (1992).
15. Agnès Chartier and Joseph Georges, ''Comparison of coaxial-beam and crossed-beam CW-laser thermal lens spectrometries for the analysis of small volume samples,'' *Anal. Meth. Instrument.* **1**, 223–228, (1993).
16. H. J. Tarigan, P. Neill, C. K. Kenmore, and D. J. Bornhop, ''Capillary-scale refractive index detection by interferometric backscatter,'' *Anal. Chem.* **68**, 1762–1770 (1996).
17. Y. Mechref and Z. E. Rassi, ''Capillary electrophoresis of herbicides,'' *Anal. Chem.* **68**, 1771–1777 (1996).
18. S. Terabe, K. Otsuka, K. Ichikawa, A. Tsuchiya, and T. Ando, ''Electrokinetic separations with micellar solutions and open-tubular capillaries,'' *Anal. Chem.* **56**, 111–113 (1984).